Chapter 5

Aquaporin Biomimetic Membranes

Amira Abdelrasoul, Huu Doan and Ali Lohi

Additional information is available at the end of the chapter

http://dx.doi.org/10.5772/intechopen.71722

Abstract

Recent research looked at an array of aquaporin protein structures, their unique functions, and potential applications in the research and industrial sectors. This chapter focuses on the specific functional features of aquaporin biomimetic membranes to interrogate their permeability properties in relation to various biomimetic water-transporting membranes. This chapter discusses in detail functional characteristics of aquaporin, how to produce it, and the status of aquaporin development.

Keywords: aquaporin, function, permeability, protein, membrane design

1. Introduction

A series of recent reviews looked at an array of aquaporin protein structures, their unique functions, and potential applications in the research and industrial sectors [1–5]. This chapter focuses on the specific functional features of aquaporin biomimetic membranes to interrogate their permeability properties in relation to various biomimetic water-transporting membranes.

Aquaporin protein structures are a family of 24–30 kDa pores that form an essential type of membrane proteins. The process of red blood cell membrane protein purification (channel-forming key membrane protein of 28 kDa or CHIP28) [6] and consequent form of this protein in *Xenopus oocytes* [7] and liposomes [8] showcased a rather quick water diffusion process along the osmotic gradients. Since this process of purification, new research data had become available on this specific class of proteins, and a term aquaporins came to define it [9]. The primary aquaporin sequence features two repetitions where each one includes three transmembrane spanning α–helices (TM 1–3), as shown in **Figure 1**. Every repetition section includes a loop between TM2 and TM3 and an asparagine-proline-alanine (NPA) pattern signature.

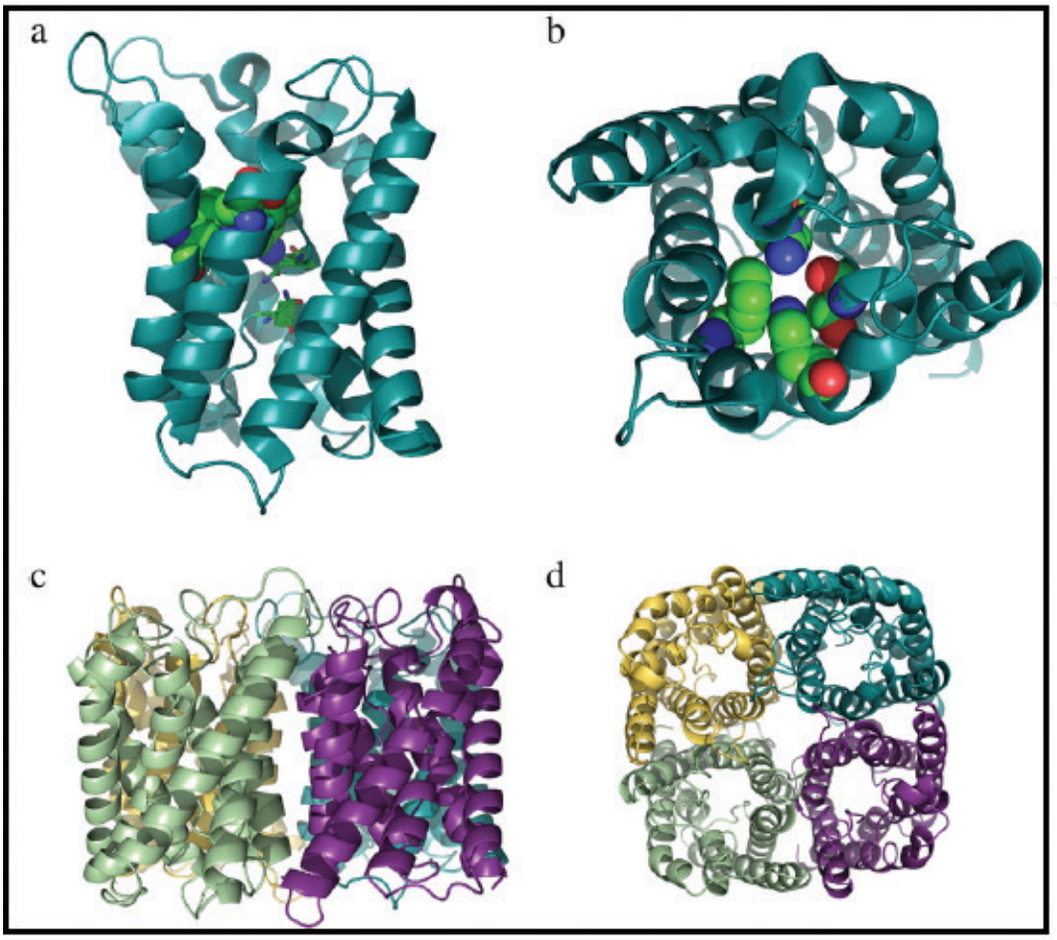

Figure 1. Aquaporin protein structure. (a): Side view of AqpZ monomer. Protein backbone (deep teal) with the two terminal asparagines from the NPA motifs shown using stick representation and the ar/R selectivity filter residues displayed in space fill representation. For stick and space fill representations, atoms have been color-coded as follows: carbon (green), oxygen (red), and nitrogen (blue). (b): Top view illustrating the selectivity filter (or constriction site) created by the four amino acids: F43, H174, R189, and T183. (c–d): Side and top view of the tetrameric AqpZ complex with the four monomers depicted in deep teal, violet purple, pale green, and yellow [1].

The aquaporin protein is assembled in a form of a hour-glass-shaped structure with six TM segments encircling a pore structure in the center and demarcated by the two opposing NPA motifs, as reflected in **Figure 1a** and **b**. The conserved aromatic/arginine (ar/R) region effectually describes the selectivity filter or constriction site, which is channel lumen's the narrowest part. The six TM AQP unit becomes a functional entity that acts as a pore, with the predominant unit assembly in biological membranes as a tetrameric arrangement [10], as indicated in **Figure 1c** and **d**. Due to their specific permeability properties, the mammalian homologs are categorized into two factions of aquaglyceroporins and aquaporins. The *Escherichia coli* model system can include both of these variants [11], the orthodox 'water only' channel AqpZ [12, 13], and the aquaglyceroporin GlpF, which is likewise permeable to glycerol [14]. While certain aquaporins may be categorized as solely water channels (e.g., AQP0, AQP4, and AqpZ), research that is being currently conducted indicates that a high number of aquaporins can have supplementary permeability properties [4].

Supplementing their already complex permeability profile parameters, multiple aquaporins showed a number of gating forms comparable to the opening and closing dynamics occurring in ion channels induced by external stimuli [15]. While numerous aspects of aquaporin gating and the process of regulating their permeability capacity remain unknown, the overall functionality of certain aquaporins has been confirmed as contingent on calmodulin [16, 17], phosphorylation, [18, 19] and pH [16, 20, 21].

2. Functional characterization of aquaporins

The properties of water's permeability and solute's rejection of single aquaporins cannot be measured very easily. Molecular dynamic simulations conducted with aquaporins suggest diffusional water permeabilities that correspond to the transport of 10^8–10^9 water molecules/s [22]. With regard to the quantity of the transported molecules, this data is about an order of magnitude greater than the parameters available in standard ion channel, with a single channel at a picoampere (pA) current level and a millisecond (ms) time scale corresponding to the transmembrane displacement of ~10^7 ions [23]. Although currents in the pA range can be calculated using the standard patch-clamp methods, the movement of 10^8–10^9 water molecules is not experimentally available due to the limitations of methods presently available to researchers. On the other hand, the macroscopic transport mediated with the aid of an ensemble of aquaporins can be measured. After this assessment is applied, the measured osmotic transport arising from a large (known) number of aquaporins can help estimate the single aquaporin permeability values. The two methods currently implemented for these calculations are as follows: *Xenopus oocyte* volume change, and light scattering from the proteoliposomes/proteopolymersomes.

In the *Xenopus oocyte* method expression, frog oocytes (~1 mm diameter) are cytoplasmically injected with mRNA that has been transcribed in vitro from a cDNA clone [24]. For aquaporins, in this instance, the resultant expression makes the oocyte membrane substantially more water permeable in comparison to the control oocytes [7]. During an osmotic challenge, the oocyte will alter its size (diameter value) and by implementing small osmotic gradients for brief period of time (e.g., 2.5 number of milliosmoles (mosM) for 5 s), the transport parameters (solute rejection and water permeability) can be calculated based on the initial rate of oocyte volume change rates in terms of shrinkage and swelling experimental runs [25].

Water permeability values of proteoliposomes/proteopolymersomes could likewise be assessed through the process of identifying the light scattering of the preparations within a stopped-flow apparatus setup, as indicated in **Figure 2a**. A suspension of aquaporin-containing vesicles of an original diameter approximately 200 nm briskly mixed with an identical volume of hyperosmolar solution featuring membrane impermeable solutes (e.g., sorbitol, sucrose, or mannitol) for proteoliposomes can create a dynamic where the subsequent transmembrane osmotic gradient will create water efflux from vesicles. As a result, the vesicle volume is lowered and may be measured with the help of an increase in the intensity values of scattered light. The rate constant, k, of the surge in normalized light intensity values is symptomatic of the water permeability coefficient and the water efflux rate constant. In this

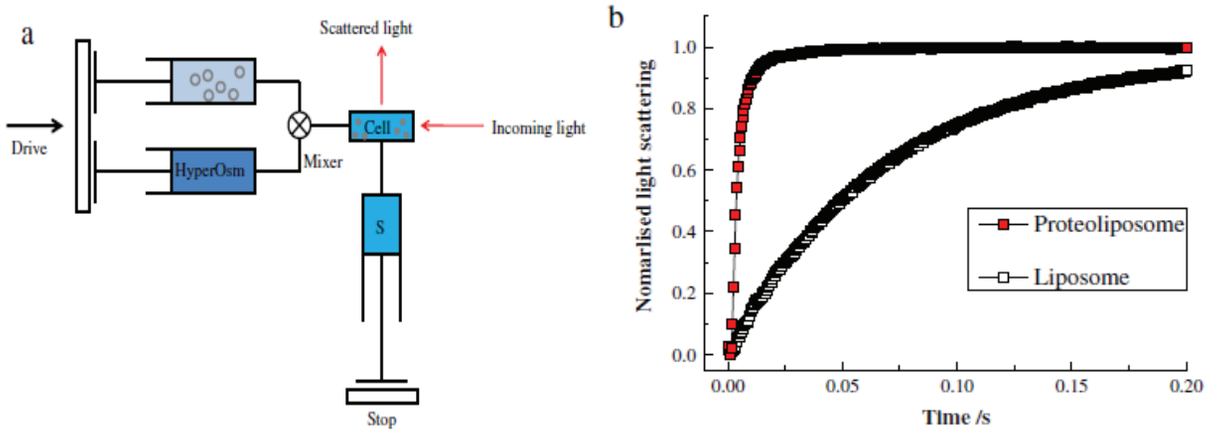

Figure 2. Stopped-flow characterization. (a) Schematics of stopped-flow measurement; (b): Typical stopped-flow values for lipid vesicles with (i.e., proteoliposomes) and without incorporated aquaporin (i.e., liposomes) [26].

instance, the light intensity values increase in an exponential manner with time, as indicated in **Figure 2b**. The response from the protein-free controls is connected to a single exponential, while the double-exponential function is applied for proteoliposomes/proteopolymersomes (vesicles) reflecting the dual pathways for water transport, either protein mediated or membrane mediated. Based on these processes, the k values can then be implemented for the calculation of the osmotic permeability P_f:

$$P_f = \frac{k}{\frac{S}{V_0} . V_w . \Delta osm}$$

where S/V_0 is the surface area of the initial volume ratio of the vesicle, V_w is the partial molar volume of water (18 cm^3/mol), and Δosm is the variance in osmolarity between the intravesicular and extravesicular aqueous solutions. Based on stopped-flow measurements, the water permeability of AqpZ is predicted to be in the range of 2–10 × 10^{-14} cm^3/s [27–29] and showed a reasonable agreement with previously reported molecular dynamics simulation results (3–30 × 10^{-14} cm^3/s).

3. Production of aquaporins

Currently, the majority of recombinant aquaporins have only been created in lab-scale quantities for the purposes of screening, regulatory, functional, or structural research studies [30, 31]. The primary concern in protein production is that the membrane protein overexpression in vivo is problematized by their overly complex structure, hydrophobic transmembrane regions with host toxicity, and the low efficiency and time-consuming refolding steps necessary. Advances in high-expression systems and their potential applications could offer an insight into how a large-scale AQP production and implementation could be facilitated. These high-expression systems include *E. coli, Pichia pastoris*, *Saccharomyces cerevisiae,* and *baculovirus*/insect cell-based systems, and their recent review is available for additional information [32].

The *E. coli* expression-based methodologies that produce milligram quantities of protein have been effectively used to analyze the X-ray structure of the AqpZ and GlpF channels, AqpZ [13], GlpF [14], and of the archaeal aquaporin AqpM [33]. A high level of expression (200 mg/L) of the traditional aquaporin AqpZ was achieved in a recent study of the *E. coli* system, where a maltose binding protein (MBP) was used as a fusion partner protein, followed by a condition optimization process [34]. The *S. cerevisiae* system can be utilized for the production of large amounts of functional aquaporins [30, 35–39]. Alternatively, the methylotrophic yeast *P. pastoris* has been effectively used to produce a high number of distinct aquaporins. The potentially produced selection includes all 13 human aquaporins [40] and a wide range of active plant aquaporins [41–47]. Large-scale expressions of various functional recombinant aquaporins have been obtained with the aid of a baculovirus/insect cell system [48–55].

Research data indicate that there is a possibility for high-level membrane protein expression based on cell-free (CF) type of production. The essential requirement in this case is the process of synthesizing membrane proteins together with natural or synthetic lipids, as well as detergents, that can help solubilize the membrane's protein content. CF type of aquaporin production has been illustrated at analytical levels [31, 56–58], and recent tests showed high expression of properly folded AqpZ. Furthermore, plant aquaporin has been achieved with *E. coli* CF protocols and implementing various fusion vectors [59, 60]. Milligram of high potential AqpZ have been created in synthetic liposomes by using a CF approach [61]. Sutro Biopharma Inc. [62] showed the possibility of cost-effective cell-free protein synthesis in a 100-l reaction and the implicit advantages offered by CF systems that can act as an effective recombinant protein in industrial-scale production platforms.

The protein, that has been stabilized using a detergent, must be modified into its host biomimetic membrane; however, this creates challenges for industrial scaling and production. These challenges may be defined in terms of the detergent-stabilized intermediates, where the detergent cost and stability become primary concerns [63, 70]. Alternatively, the process of optimizing the interaction between membrane, protein (c.f. [64–66]), and yield may directly affect how much of functional protein content can be integrated into the final product (c.f. [67]).

4. Status of the aquaporin membrane development

Research conducted by Tang et al. suggests that membranes with excessively high salt rejection and permeability values can be created with the aid of aquaporin protein [68]. The measured water permeability values of AqpZ with proteoliposomes are used by researchers to argue that AqpZ-based biomimetic membranes can, in theory, obtain a membrane permeability as high as 167 $\mu m \cdot s^{-1} \cdot bar^{-1}$ (i.e., 601 $L \cdot m^{-2} \cdot h^{-1} \cdot bar^{-1}$, as shown in **Figure 3**). This value is more permeable by about two orders of magnitude when compared to the preexisting commercially available seawater RO membranes [69]. Even though there is a high level of membrane permeability present, there are considerable scaled-up concerns remaining. This is primarily due to the fact that the membranes are built using nanoscale elements, that is, aquaporins, and there are serious questions about how the biomimetic membranes can be scaled up and then stabilized to about 1 m^2 dimensions appropriate for industrial applications.

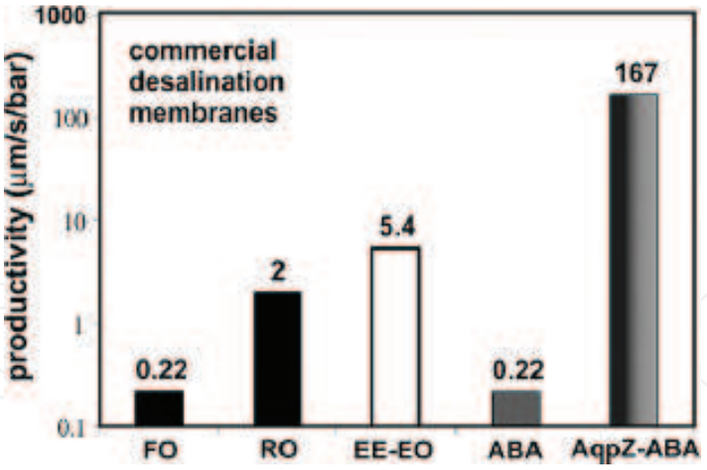

Figure 3. Comparison of water permeability of polymer vesicles with AqpZ (AqpZ-ABA) and without AqpZ (ABA) to those present in polymeric membranes [69].

Multiple design methods have been planned for the foreseeable future, as outlined in **Figure 4**. These strategies incorporate the creation of membranes based across multiple micron scale apertures, possibly as freestanding lipid or polymer membranes [44, 53, 68, 69], or alternatively as membranes stabilized using polymeric support materials [70]. Additional methods depend on nanoporous support materials on top of which the membranes are placed. For example, in this approach, there are several variations. The charged lipid vesicle can be deposited onto the commercially available nanofiltration membranes where the recipient surface is either a crosslinked polyamide or a sulfonated polysulfone negatively charged at pH7 [71]; there is an active rupture of aquaporin-containing polymersomes on top of the methacrylate functionalized cellulose acetate membranes [72], the method where detergent-stabilized tagged aquaporin are introduced into monolayers with nickel-chelating lipids [73]; and proteopolymersome deposition onto the surface of polycarbonate track-etched substrates covered with gold and then functionalized using photoactive acrylate groups. Research data suggest that [71–73] the implementation of spin coating and applied pressure improves vesicular coating/fusion on the substrate. As part of this process, surface charge and hydrophilicity values have been proven to play an essential role in shaping the overall quality of the supported lipid layers.

The data outlined in **Table 1** show the existing methods of creating aquaporin-based biomimetic membranes. In the majority of cases, most of the membranes discussed earlier feature a relatively low NaCl rejection value (or the rejection information is not available), a dynamic that prevents them from being used in desalination processes. Moreover, a large number of these membranes are not sufficiently stable for sophisticated industrial applications. In most cases, only small membrane areas are prepared, and the majority of methods depend on the implementation of specialized nanofabrication approaches, making the process exceedingly complicated and excessively expensive for scale up in forward osmosis (FO) and RO membrane fabrication. Ongoing innovation has allowed for the development of a new approach in the process of fabricating aquaporin-based biomimetic membranes. This innovative method relies on embedding aquaporin-containing proteopolymersomes or proteoliposomes into a

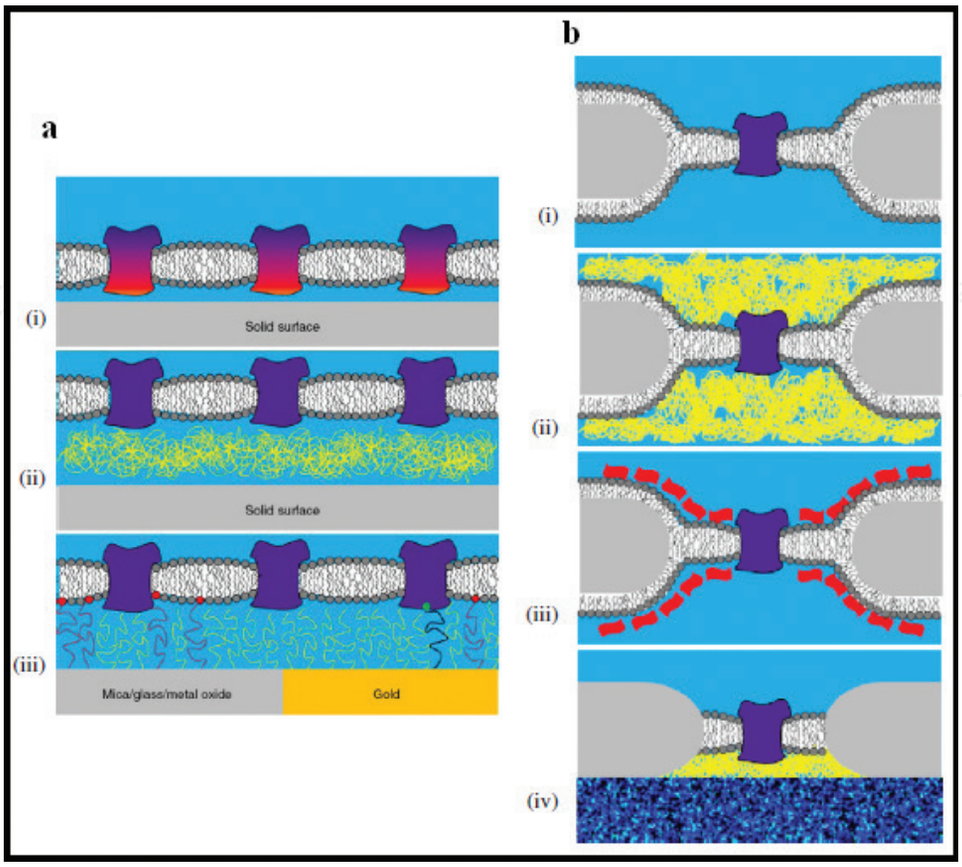

Figure 4. Summary of the existing biomimetic membrane designs. (a): Cross-sectional examples of solid-supported biomimetic membranes. (i) Direct deposition on a hydrophilic surface (light gray). This technique may introduce part of the integral membrane proteins (red protein shaded areas) embedded in the matrix formed from the self-assembly of lipids (dark gray molecules) too close to the surface, potentially inactivating (or even denaturing) the protein. (ii) Cushion-supported biomimetic membrane. (iii) Layers grafted covalently onto the support using spacers with silane groups and reacting with hydroxyl surfaces (light gray), or spacers with thiol groups bonding on gold surfaces (orange). Various hydrophilic spacers (e.g., poly(ethylene glycol) (PEG)) may be applied as cushion material. This cushion can be noncovalently interacting with the biomimetic membrane (yellow spacers) or covalently attached to lipids (red lipid headgroups) or proteins (green bonds), in the biomimetic membrane directly or through intermediates, for example, biotin-avidin complexes. (b): Cross-sectional illustrations of porous supported biomimetic membranes with an embedded protein (blue). (i) Freestanding membrane formed across a (micro or nano) porous support section. The membrane (solvent-free or solvent-containing) is formed in an aperture (light gray). (ii) Hydrogel-encapsulated biomimetic membrane. A hydrogel polymer meshwork (yellow) encapsulating the biomimetic membrane. (iii) A surface (S) layer-encapsulated membrane. The monomolecular layer of protein or glycoproteins (red) self-assembles into a two-dimensional lattice creating identical pores 2–8 nm in diameter. (iv) A cushioned membrane on a porous support [70, 71].

crosslinked polyamide matrix [69, 71]. In this approach, a microporous substrate was first soaked in an aqueous solution of m-phenylene-diamine (MPD) that likewise includes some aquaporin-containing vesicles, as shown in **Figure 4**. These soaked substrates were subsequently exposed to a tri-mesoyl chloride (TMC) solution to allow the formation of an interfacially polymerized polyamide rejection layer with vesicles dispersed in a thin rejection layer.

As part of this design, the aquaporin-containing vesicles offer superior water pathways through the polyamide layer and as a result substantially improve the membrane's water capacity for permeability. Furthermore, the crosslinked polyamide provides a scaffold that maintains the

Approach	WP ($L \cdot m^{-1} \cdot h^{-1} \cdot bar^{-1}$)	RNaCl (%)	Area (cm^2)	P_{max} (bar)	Upscaling issues	Remarks	Ref.
Charged lipid mixture vesicles depositions onto NF membranes	0.83	n.d.	3.5	10	Difficult to produce large defect-free membranes	No aquaporin incorporated	[11]
Vesicle fusion facilitated by hydraulic pressure on hydrophilic NF membranes coated with positively charged lipids	3.6 ± 0.2	35 ± 8	12.6	1	Difficult to produce large defect-free membranes	Low R_{NaCl}. Only suitable for NF. WP/RNaCl not tested. Not	[67]
Membranes across multiple micron scale apertures either as free-standing lipid or polymer membranes	n.d.	n.d.	4[a]	n.d.	Nanofabrication required Low robustness	WP/RNaCl not tested. Not suitable for RO.	[66, 67]
Membranes across multiple micron scale apertures and stabilized by hydrogel encapsulation	12–40	n.d.	3.5[a]	2	Nanofabrication required. High robustness	Characterized with gramicidin channels. No aquaporin incorporated.	[18]
Aquaporin containing polymersomes on methacrylate functionalized CA membranes	34.2 ± 6.9	32.9 ± 9.1	0.07	5	Medium robustness	Small area. High WP but low R_{NaCl}. Only suitable for NF.	[17]
Detergent-stabilized His-tagged aquaporin added to monolayers with nickel-chelating lipids	n.d.	n.d.	n.d.	n.d.	Complex fabrication. Low robustness	WP/RNaCl not tested. May not be suitable for desalination.	[51]
Proteopolymersome deposition onto gold-functionalized PC track-etched substrates	n.d.[b]	n.d.[b]	0.096	n.d.	Complex fabrication. Low robustness	Small area. Relatively high WP in FO. No RO data.	[35]
Interfacial polymerization method with embedded proteoliposomes	4 ± 0.4	96.3 ± 1.2	>200	14	Simple fabrication. High robustness	Combined high WP and RNaCl. Suitable for RO.	[8]

[a]Including membrane scaffold.

[b]RO tests were not performed. Based on FO tests, a WP of 16.4 $L \cdot m^{-2} \cdot h^{-1}$ and a salt flux of 6.6 $g \cdot m^{-2} \cdot h^{-1}$ were obtained for membranes prepared with a protein-to-polymer molar ratio of 1:100, with 0.3 M sucrose as draw and 200 ppm NaCl as feed.

Table 1. Existing approaches for the preparation of aquaporin-based biomimetic membranes. Performance data are presented as water permeability (WP) [$L \cdot m^{-2} \cdot h^{-1} \cdot bar^{-1}$], NaCl rejection (RNaCl) [%], membrane area (A) [cm^2], and maximal external pressure applied (PMax) [bar] when operated in RO. CA: cellulose acetate, PC: polycarbonate.

aquaporin-containing vesicles as well as defends them against the surrounding environmental conditions. This dynamic is anticipated to considerably increase the membrane's overall stability. This type of membrane exhibited a permeability value of ~4 $L \cdot m^{-2} \cdot h^{-1} \cdot bar^{-1}$, as shown in **Table 1**, while maintaining similar or even superior NaCl rejection values. This permeability is ~40% greater than the one occurring in commercial brackish water reverse osmosis membrane BW30 that was tested in the same conditions. Membranes featuring such a design have been extensively tested and showed enhanced stable flux and rejection performance capacity for the specified durations of weeks and months. A noticeable water improvement effect of aquaporins was likewise confirmed through a comparative analysis with membranes featuring vesicles containing inactive R189A AqpZ mutants [69–71]. This straightforward quality of this fabrication procedure ensures that this technique can be effortlessly scaled up for the manufacturing of large membrane areas crucial for industrial applications.

Author details

Amira Abdelrasoul[1]*, Huu Doan[2] and Ali Lohi[2]

*Address all correspondence to: amira.abdelrasoul@usask.ca

1 Department of Chemical and Biological Engineering, University of Saskatchewan, Saskatoon, Saskatchewan, Canada

2 Department of Chemical Engineering, Ryerson University, Toronto, Ontario, Canada

References

[1] Gonen T, Walz T. The structure of aquaporins. Quarterly Reviews of Biophysics. 2006; **39**:361-396

[2] Fu D, Lu M. The structural basis of water permeation and proton exclusion in aquaporins. Molecular Membrane Biology. 2007;**24**:366-374

[3] Ishibashi K. Aquaporin subfamily with unusual NPA boxes. Biochimica et Biophysica Acta. 2006;**1758**:989-993

[4] Verkman AS. More than just water channels: Unexpected cellular roles of aquaporins. Journal of Cell Science. 2005;**118**:3225-3232

[5] Nielsen S, Frokiaer J, Marples D, Kwon TH, Agre P, Knepper MA. Aquaporins in the kidney: From molecules to medicine. Physiological Reviews. 2002;**82**:205-244

[6] Denker BM, Smith BL, Kuhajda FP, Agre P. Identification, purification, and partial characterization of a novel Mr 28,000 integral membrane protein from erythrocytes and renal tubules. The Journal of Biological Chemistry. 1988;**263**:15634-15642

[7] Preston GM, Carroll TP, Guggino WB, Agre P. Appearance of water channels in Xenopus oocytes expressing red cell CHIP28 protein. Science. 1992;**256**:385-387

[8] Zeidel ML, Ambudkar SV, Smith BL, Agre P. Reconstitution of functional waterchannels in liposomes containing purified red cell CHIP28 protein. Biochemistry. 1992;**31**: 7436-7440

[9] Agre P, Sasaki S, Chrispeels MJ. Aquaporins: A family of water channel proteins. The American Journal of Physiology. 1993;**265**:F461

[10] Verbavatz JM, Brown D, Sabolic I, Valenti G, Ausiello DA, Van Hoek AN, Ma T, Verkman AS. Tetrameric assembly of CHIP28 water channels in liposomes and cell membranes: A freeze-fracture study. The Journal of Cell Biology. 1993;**123**:605-618

[11] Borgnia MJ, Agre P. Reconstitution and functional comparison of purified GlpF and AqpZ, the glycerol and water channels from *Escherichia coli*. Proceedings of the National Academy of Sciences of the United States of America. 2001;**98**:2888-2893

[12] Calamita G, Bishai WR, Preston GM, Guggino WB, Agre P. Molecular cloning and characterization of AqpZ, a water channel from *Escherichia coli*. The Journal of Biological Chemistry. 1995;**270**:29063-29066

[13] Savage DF, Egea PF, Robles-Colmenares Y, O'Connell JD 3rd, Stroud RM. Architecture and selectivity in aquaporins: 2.5 a X-ray structure of aquaporin Z. PLoS Biology. 2003;**1** E72

[14] Fu D, Libson A, Miercke LJ, Weitzman C, Nollert P, Krucinski J, Stroud RM. Structure of a glycerol-conducting channel and the basis for its selectivity. Science. 2000;**290**: 481-486

[15] Xin L, Su H, Nielsen CH, Tang C, Torres J, Mu Y. Water permeation dynamics of AqpZ: A tale of two states. Biochim. Biophys. Acta. 2011;**1808**:1581-1586

[16] Nemeth-Cahalan KL, Hall JE. pH and calcium regulate the water permeability of aquaporin 0. The Journal of Biological Chemistry. 2000;**275**:6777-6782

[17] Nemeth-Cahalan KL, Kalman K, Hall JE. Molecular basis of pH and Ca2+ regulation of aquaporin water permeability. The Journal of General Physiology. 2004;**123**:573-580

[18] Johansson I, Larsson C, Ek B, Kjellbom P. The major integral proteins of spinach leaf plasma membranes are putative aquaporins and are phosphorylated in response to Ca2+ and apoplastic water potential. Plant Cell. 1996;**8**:1181-1191

[19] Johansson I, Karlsson M, Shukla VK, Chrispeels MJ, Larsson C, Kjellbom P. Water transport activity of the plasma membrane aquaporin PM28A is regulated by phosphorylation. Plant Cell. 1988;**10**:451-459

[20] Zeuthen T, Klaerke DA. Transport of water and glycerol in aquaporin 3 is gated by H(+). The Journal of Biological Chemistry. 1999;**274**:21631-21636

[21] Yasui M, Hazama A, Kwon TH, Nielsen S, Guggino WB, Agre P. Rapid gating and anion permeability of an intracellular aquaporin. Nature. 1999;**402**:184-187

[22] Jensen MO, Mouritsen OG. Single-channel water permeabilities of *Escherichia coli* aquaporins AqpZ and GlpF. Biophysical Journal. 2006;**90**:2270-2284

[23] Hille B. Ionic Channels of Excitable Membranes. Sunderland: Sinauer; 2001

[24] Gurdon JB, Lane CD, Woodland HR, Marbaix G. Use of frog eggs and oocytes for the study of messenger RNA and its translation in living cells. Nature. 1971;**233**:177-182

[25] Meinild AK, Klaerke DA, Zeuthen T. Bidirectional water fluxes and specificity for small hydrophilic molecules in aquaporins 0-5. The Journal of Biological Chemistry. 1998; **273**:32446-32451

[26] Borgnia MJ, Kozono D, Calamita G, Maloney PC, Agre P. Functional reconstitution and characterization of AqpZ, the *E. coli* water channel protein. Journal of Molecular Biology. 1999;**291**:1169-1179

[27] Scheuring S, Ringler P, Borgnia M, Stahlberg H, DJM l, Agre P, Engel A. High resolution AFM topographs of the *Escherichia coli* water channel aquaporin Z. The EMBO Journal. 1999;**18**:7

[28] Mathai JC, Tristram-Nagle S, Nagle JF, Zeidel ML. Structural determinants of water permeability through the lipid membrane. The Journal of General Physiology. 2008;**131**:8

[29] Hovijitra NT, Wuu JJ, Peaker B, Swartz JR. Cell-free synthesis of functional aquaporin Z in synthetic liposomes. Biotechnol. Bioengineering. 2109;**4**:10

[30] Kaldenhoff R, Bertl A, Otto B, Moshelion M, Uehlein N. Characterization of plant aquaporins. Methods in Enzymology. 2007;**428**:505-531

[31] Shi LB, Skach WR, Ma T, Verkman AS. Distinct biogenesis mechanisms for the water channels MIWC and CHIP28 at the endoplasmic reticulum. Biochemistry. 1995;**34**:8250-8256

[32] Altamura N, Calamita G. Systems for production of proteins for biomimetic membrane devices. In: Hélix-Nielsen C, editor. Biomimetic Membranes for Sensor and Separation Applications. Dordrecht: Springer; 2012. p. 233-250

[33] Lee JK, Kozono D, Remis J, Kitagawa Y, Agre P, Stroud RM. Structural basis for conductance by the archaeal aquaporin AqpM at 1.68 A. Proceedings of the National Academy of Sciences of the United States of America. 2005;**102**:18932-18937

[34] Lian J, Ding S, Cai J, Zhang D, Xu Z, Wang X. Improving aquaporin Z expression in *Escherichia coli* by fusion partners and subsequent condition optimization. Applied Microbiology and Biotechnology. 2009;**82**:463-470

[35] Bienert GP, Moller AL, Kristiansen KA, Schulz A, Moller IM, Schjoerring JK, Jahn TP. Specific aquaporins facilitate the diffusion of hydrogen peroxide across membranes. The Journal of Biological Chemistry. 2007;**282**:1183-1192

[36] Fischer G, Kosinska-Eriksson U, Aponte-Santamaria C, Palmgren M, Geijer C, Hedfalk K, Hohmann S, de Groot BL, Neutze R, Lindkvist-Petersson K. Crystal structure of a yeast aquaporin at 1.15 angstrom reveals a novel gating mechanism. PLoS Biology 2009;**7**: e1000130

[37] Hedfalk K, Pettersson N, Oberg F, Hohmann S, Gordon E. Production, characterization and crystallization of the *Plasmodium falciparum* aquaporin. Protein Expression and Purification. 2008;**59**:69-78

[38] Laize V, Ripoche P, Tacnet F. Purification and functional reconstitution of the human CHIP28 water channel expressed in *Saccharomyces cerevisiae*. Protein Expression and Purification. 1997;**11**:284-288

[39] Pettersson N, Hagstrom J, Bill RM, Hohmann S. Expression of heterologous aquaporins for functional analysis in *Saccharomyces cerevisiae*. Current Genetics. 2006;**50**:247-255

[40] Oberg F, Ekvall M, Nyblom M, Backmark A, Neutze R, Hedfalk K. Insight into factors directing high production of eukaryotic membrane proteins; production of 13 human AQPs in *Pichia pastoris*. Molecular Membrane Biology. 2009;**26**:215-227

[41] Azad AK, Katsuhara M, Sawa Y, Ishikawa T, Shibata H. Characterization of four plasma membrane aquaporins in tulip petals: A putative homolog is regulated by phosphorylation. Plant Cell Physiol. 2008;**49**:1196-1208

[42] Azad AK, Sawa Y, Ishikawa T, Shibata H. Heterologous expression of tulip petal plasma membrane aquaporins in *Pichia pastoris* for water channel analysis. Applied and Environmental Microbiology. 2009;**75**:2792-2797

[43] Daniels MJ, Wood MR, Yeager M. In vivo functional assay of a recombinant aquaporin in *Pichia pastoris*. Applied and Environmental Microbiology. 2006;**72**:1507-1514

[44] Karlsson M, Fotiadis D, Sjovall S, Johansson I, Hedfalk K, Engel A, Kjellbom P. Reconstitution of water channel function of an aquaporin overexpressed and purified from *Pichia pastoris*. FEBS Letters. 2003;**537**:68-72

[45] Kukulski W, Schenk AD, Johanson U, Braun T, de Groot BL, Fotiadis D, Kjellbom P, Engel A. The 5A structure of heterologously expressed plant aquaporin SoPIP2;1. Journal of Molecular Biology 2005;**350**:611-616.

[46] Tornroth-Horsefield S, Wang K, Hedfalk Y, Johanson U, Karlsson M, Tajkhorshid E, Neutze R, Kjellbom P. Structural mechanism of plant aquaporin gating. Nature. 2006;**439**: 688-694

[47] Verdoucq L, Grondin A, Maurel C. Structure-function analysis of plant aquaporin AtPIP2;1 gating by divalent cations and protons. The Biochemical Journal. 2008;**415**:409-416

[48] Yang B, van Hoek AN, Verkman AS. Very high single channel water permeability of aquaporin-4 in baculovirus-infected insect cells and liposomes reconstituted with purified aquaporin-4. Biochemistry. 1997;**36**:7625-7632

[49] Swamy-Mruthinti S, Schey KL. Mass spectroscopic identification of in vitro glycated sites of MIP. Current Eye Research. 1997;**16**:936-941

[50] Werten PJ, Hasler L, Koenderink JB, Klaassen CH, de Grip WJ, Engel A, Deen PM. Large-scale purification of functional recombinant human aquaporin-2. FEBS Letters 2001;**504**: 200-205

[51] Drake KD, Schuette D, Chepelinsky AB, Crabbe MJ. Heterologous expression and topography of the main intrinsic protein (MIP) from rat lens. FEBS Letters 2002;**512**:191-198

[52] Drake KD, Schuette D, Chepelinsky AB, Jacob TJ, Crabbe MJ. pH-Dependent channel activity of heterologously-expressed main intrinsic protein (MIP) from rat lens. FEBS Letters. 2002;**512**:199-204

[53] Hiroaki Y, Tani K, Kamegawa A, Gyobu N, Nishikawa K, Suzuki H, Walz T, Sasaki S, Mitsuoka K, Kimura K, Mizoguchi A, Fujiyoshi Y. Implications of the aquaporin-4 structure on array formation and cell adhesion. Journal of Molecular Biology. 2006;**355**:628-639

[54] Yakata K, Hiroaki Y, Ishibashi K, Sohara E, Sasaki S, Mitsuoka K, Fujiyoshi Y. Aquaporin-11 containing a divergent NPA motif has normal water channel activity. Biochimica et Biophysica Acta. 2007;**1768**:688-693

[55] Hayakawa S, Mori M, Okuta A, Kamegawa A, Fujiyoshi Y, Yoshiyama Y, Mitsuoka K, Ishibashi K, Sasaki S, Hattori T, Kuwabara S. Neuromyelitis optica and anti-aquaporin-4 antibodies measured by an enzyme-linked immunosorbent assay. Journal of Neuroimmunology. 2008;**196**:181-187

[56] LaVallie ER, Lu Z, Diblasio-Smith EA, Collins-Racie LA, JM MC. Thioredoxin as a fusion partner for production of soluble recombinant proteins in *Escherichia coli*. Methods in Enzymology. 2000;**326**:322-340

[57] Lu Y, Turnbull IR, Bragin A, Carveth K, Verkman AS, Skach WR. Reorientation of aquaporin-1 topology during maturation in the endoplasmic reticulum. Molecular Biology of the Cell. 2000;**11**:2973-2985

[58] Paul DL, Goodenough DA. In vitro synthesis and membrane insertion of bovine MP26, an integral protein from lens fiber plasma membrane. The Journal of Cell Biology. 1983;**96**:633-638

[59] Xu Z, Lian J, Cai J. Efficient expression of aquaporin Z in *Escherichia coli* cell-free system using different fusion vectors. Protein and Peptide Letters. 2010;**17**:181-185

[60] Schwarz D, Junge F, Durst F, Frolich N, Schneider B, Reckel S, Sobhanifar S, Dotsch V, Bernhard F. Preparative scale expression of membrane proteins in *Escherichia coli*-based continuous exchange cell-free systems. Nature Protocols. 2007;**2**:2945-2957

[61] Hovijitra NT, Wuu JJ, Peaker B, Swartz JR. Cell-free synthesis of functional aquaporin Z in synthetic liposomes. Biotechnology and Bioengineering. 2009;**104**:40-49

[62] Zawada JF, Yin G, Steiner AR, Yang J, Naresh A, Roy SM, Gold DS, DS HHG, Murray CJ. Microscale to manufacturing scale-up of cell-free cytokine production—a new approach for shortening protein production development timelines. Biotechnology and Bioengineering. 2011;**108**:1570-1578

[63] Hansen JS, Vararattanavech A, Plasencia I, Greisen PJ, Bomholt J, Torres J, Emneus J, Helix-Nielsen C. Interaction between sodium dodecyl sulfate and membrane reconstituted aquaporins: A comparative study of spinach SoPIP2;1 and *E. coli* AqpZ. Biochimica et Biophysica Acta. 2011;**1808**:2600-2607

[64] Plasencia I, Survery S, Ibragimova S, Hansen JS, Kjellbom P, Helix-Nielsen C, Johanson U, Mouritsen OG. Structure and stability of the spinach aquaporin SoPIP2;1 in detergent micelles and lipid membranes. PLoS One. 2011;**6**:e14674

[65] Andersen OS, Nielsen C, Maer AM, Lundbæk JA, Goulian M, Koeppe RE. Ion channels as tools to monitor lipid bilayer–membrane protein interactions: gramicidin channels as molecular force transducers, Methods Enzymol. 1999;**294**:208-224

[66] Nielsen C, Goulian M, Andersen OS. Energetics of inclusion-induced bilayer deformations. Biophysical Journal. 1998;**74**:1966-1983

[67] Pszon-Bartosz K, Hansen JS, Stibius KB, Groth JS, Emneus J, Geschke O, Helix-Nielsen C. Assessing the efficacy of vesicle fusion with planar membrane arrays using a mitochondrial porin as reporter. Biochemical and Biophysical Research Communications. 2011;**406**:96-100

[68] Tang CY, Wang Z, Petrinic I, Fane AG, Hélix-Nielsen C. Biomimetic aquaporin membranes coming of age. Desalination. 2015;**368**:89-105

[69] Tang CY, Zhao Y, Wang R, Hélix-Nielsen C, Fane AG. Desalination by biomimetic aquaporin membranes: Review of status and prospects. Desalination. 2013;**308**:34-40

[70] Lander MR, Ibragimova S, Rein C, Vogel J, Stibius K, Geschke O, Perry M, Helix-Nielsen C. Biomimetic membrane arrays on cast hydrogel supports. Langmuir. 2011;**27**:7002-7007

[71] Kaufman Y, Grinberg S, Linder C, Heldman E, Gilron J, Freger V. Fusion of bolaamphiphile micelles: A method to prepare stable supported biomimetic membranes. Langmuir. 2013;**29**:1152-1161

[72] Zhong PS, Chung T-S, Jeyaseelan K, Armugam A. Aquaporin-embedded biomimetic membranes for nanofiltration. Journal of Membrane Science. 2012;**407**(408):27-33

[73] Zhang X, Tanner P, Graff A, Palivan CG, Meier W. Mimicking the cell membrane with block copolymer membranes. Journal of Polymer Science Part A: Polymer Chemistry. 2012;**50**:2293-2318